



HAL
open science

Highly deformed nuclei at high spin

Z. Szymanski

► **To cite this version:**

Z. Szymanski. Highly deformed nuclei at high spin. École thématique. Ecole Joliot Curie "Les noyaux en pleines formes", Maubuisson, (France), du 16-21 septembre 1991: 10ème session, 1991. cel-00648242

HAL Id: cel-00648242

<https://cel.hal.science/cel-00648242>

Submitted on 5 Dec 2011

HAL is a multi-disciplinary open access archive for the deposit and dissemination of scientific research documents, whether they are published or not. The documents may come from teaching and research institutions in France or abroad, or from public or private research centers.

L'archive ouverte pluridisciplinaire **HAL**, est destinée au dépôt et à la diffusion de documents scientifiques de niveau recherche, publiés ou non, émanant des établissements d'enseignement et de recherche français ou étrangers, des laboratoires publics ou privés.

Highly Deformed Nuclei at High Spin

Z. Szymański

*Institute of Theoretical Physics,
Warsaw University, Warsaw, Poland*

1 Elements of Physics

Rotational bands can occur in principle on top of an arbitrary quantal state of a nucleus as long, as its intrinsic structure is deformed i.e. corresponds to a nonspherical distribution of nuclear matter. In the variety of all possible nuclear shapes the axially symmetric ones are most common and best known. The energies of the rotational states in one band obey the “ $I(I+1)$ rule” i.e. the relation

$$E_I = \frac{\hbar^2}{2\mathcal{J}} I(I+1) \quad (1)$$

with angular momentum I changing in the range $I_0, I_0 + 1, I_0 + 2, \dots$ or else $I_0, I_0 + 2, I_0 + 4, \dots$ and $I_0 + 1, I_0 + 3, \dots$ if the two parts of the band are treated separately as two distinct bands. Here, I_0 is determined by the intrinsic state on top of which the band is built (often called a bandhead). The proportionality coefficient in eq. (1) defines the nuclear moment of inertia \mathcal{J} which will be discussed more extensively later.

We shall not go into the details in the physical description of rotational bands in nuclei at low angular momenta. Instead, we shall show an example of the bands in one nucleus at low energy and low angular momenta. Fig. 1.1 illustrates the low lying spectrum in the nucleus ^{232}Th . Three well developed rotational bands are built on the ground-state, the axially symmetric vibrational state 0^+ (beta vibration), and the 2^+ bandhead assigned as a nonaxial vibration (gamma vibration). The 4^+ and 6^+ bandheads may correspond to the higher vibrational excitations (ref. [1]).

A most commonly known quantal picture of the rotational states has been suggested by A.Bohr and B.R.Mottelson [2-4] in terms of a particle-rotor model. The

232 Th

<u>24°</u>	<u>3619</u>			
		<u>20°</u>	<u>3248</u>	
<u>22°</u>	<u>3144</u>			
		<u>18°</u>	<u>2831</u>	
<u>20°</u>	<u>2691.4</u>			<u>18°</u>
				<u>2766.1</u>
<u>18°</u>	<u>2262.4</u>	<u>16°</u>	<u>2440.3</u>	<u>16°</u>
				<u>2445.3</u>
		<u>14°</u>	<u>2080.3</u>	<u>14°</u>
				<u>2117.1</u>
<u>16°</u>	<u>1858.7</u>			<u>(16°)</u>
		<u>12°</u>	<u>1754.7</u>	<u>12°</u>
				<u>1801.6</u>
<u>14°</u>	<u>1482.5</u>	<u>10°</u>	<u>1467.5</u>	<u>11°</u>
				<u>-164.1</u>
				<u>10°</u>
				<u>1513.0</u>
<u>12°</u>	<u>1137.1</u>	<u>8°</u>	<u>1222.3</u>	<u>9°</u>
				<u>-137.1</u>
		<u>6°</u>	<u>1023.4</u>	<u>8°</u>
				<u>1260.7</u>
<u>10°</u>	<u>826.8</u>	<u>4°</u>	<u>873.1</u>	<u>7°</u>
				<u>-116.2</u>
		<u>2°</u>	<u>774.5</u>	<u>6°</u>
				<u>1051.2</u>
<u>8°</u>	<u>556.9</u>	<u>0°</u>	<u>730.6</u>	<u>5°</u>
				<u>960.3</u>
				<u>4°</u>
				<u>890.5</u>
<u>6°</u>	<u>333.2</u>			<u>3°</u>
				<u>829.7</u>
<u>4°</u>	<u>162.0</u>			<u>2°</u>
				<u>785.5</u>
<u>2°</u>	<u>49.4</u>	<u>0°</u>		
<u>0°</u>	<u>0</u>			

Fig. 1.1

corresponding approximate wave function has the structure of a product

$$\Psi(x) = D_{MK}^I(\alpha, \beta, \gamma)\chi_K(x') \quad (2)$$

where $x(\equiv x_1, x_2, x_3)$ refers to all coordinates fixed in space, $x'(\equiv x'_1, x'_2, x'_3)$ are coordinates related to the nuclear principal axes and (α, β, γ) denote the Euler angles between the two reference systems. Quantity $D_{MK}^I(\alpha, \beta, \gamma)$ denotes a Wigner function for finite rotations characterised by the total spin (i.e. the total angular momentum) I with M and K denoting its projections on the quantisation axes x_3 and x'_3 of the laboratory and body-fixed frames, respectively. Wave function (2) leads to the $I(I+1)$ rule described by eq. (1). There appears, however, one important exception in odd- A nuclei for $K = 1/2$ where formula (1) has to be modified. Thus a more general formula reads (cf. e.g. ref. [4]):

$$E_I = \frac{\hbar^2}{2\mathcal{J}} \left\{ I(I+1) + (-1)^{I+1/2}(I+1/2)a\delta_{K1/2} \right\} \quad (3)$$

The appearance of the second term is connected first of all with the freedom in the choice of the positive direction along the x'_3 -axis and, second, with the coupling between the $K = 1/2$ and $K = -1/2$ components by the angular momentum operator j_+ . This leads to a decoupling of the $K = 1/2$ orbit from rotation. Parameter a called the decoupling parameter can be expressed as

$$a = -\langle K = 1/2 | j_+ | \overline{K = 1/2} \rangle \quad (4)$$

the bar over the state $|\overline{K = 1/2}\rangle$ denoting time reversal.

Let us now come to the discussion of nuclear rotation in terms of the quantal structure often referred to as the intrinsic structure as contrasted to the external rotation. This is done by an approximate semiclassical procedure called the cranking model [5]. The nucleus is rotated externally with constant rotational frequency ω (i.e. angular velocity) about an axis fixed in space (say, the x_1 -axis). A relation between the nuclear Hamiltonian H and that in the rotating system of reference H^ω (called the cranking Hamiltonian) is given by classical mechanics (see e.g. ref. [6])

$$H^\omega = H - \omega J_1 \hbar \quad (5)$$

where J_1 is the component of nuclear angular momentum along the rotation axis. Eigenvalues E^ω of H^ω (called Routhians) and eigenstates $|\Psi^\omega\rangle$ describe the nucleus in a rotating system. The total angular momentum I is given in this model as

$$I = \langle \Psi^\omega | J_1 | \Psi^\omega \rangle \quad (6)$$

while the total energy

$$E = \langle \Psi^\omega | H | \Psi^\omega \rangle = E^\omega + \hbar I \omega \quad (7)$$

may be treated as function of I with ω determined by the solution of eq.(1.6) with respect to ω . Quantities ω and I are canonically conjugate i.e.

$$\hbar \omega = \frac{dE}{dI} \quad (8)$$

and

$$\hbar I = -\frac{dE^\omega}{d\omega} \quad (9)$$

Let us now observe that the rotation of the system about an x_1 -axis through an angle 180° leaves the cranking Hamiltonian invariant (if H itself has this property!). Thus an eigenvalue $r = \exp(-i\pi\alpha)$ of the operator

$$R = \exp(-i\pi J_1) \quad (10)$$

is a good quantum number. It is called signature. We have the following relations between r and the allowed angular momentum I in the band

$$\begin{aligned} r &= +1 \quad (\alpha = 0); & I &= 0, 2, 4, \dots \\ r &= -1 \quad (\alpha = 1); & I &= 1, 3, 5, \dots \\ r &= -i \quad (\alpha = 1/2); & I &= 1/2, 5/2, 9/2, \dots \\ r &= +i \quad (\alpha = -1/2); & I &= 3/2, 7/2, 11/2, \dots \end{aligned} \quad (11)$$

It is just the signature quantum number that suggests to treat the rotational band $I_0, I_0 + 1, I_0 + 2, \dots$ rather as two distinct bands with different signatures.

Let us come now to the moments of inertia. Actually two different moments of inertia may be useful in the description of bands at high angular momentum [7]. We define the kinematical moment of inertia

$$\mathcal{J}^{(1)} = I\hbar/\omega = (\hbar^2/2) \left(\frac{dE}{dI^2} \right)^{-1} \quad (12)$$

and the dynamical moment of inertia

$$\mathcal{J}^{(2)} = \hbar(dI/d\omega) = \hbar^2 \left(\frac{d^2 E}{dI^2} \right)^{-1} \quad (13)$$

Obviously, for a rigid-body rotation defined by

$$E = \frac{\hbar^2}{2\mathcal{J}_0} I^2 \quad (14)$$

both moments of inertia coincide

$$\mathcal{J}^{(1)} = \mathcal{J}^{(2)} = \mathcal{J}_0 \quad (15)$$

The behaviour of the two moments of inertia $\mathcal{J}^{(0)}$ and $\mathcal{J}^{(2)}$ along the rotational band provides a very instructive insight into the properties of nuclei rotating with high angular momentum. Below, only two examples are given. Fig. 1.2a) illustrates the behaviour in the curve of $\mathcal{J}^{(1)}$ versus ω for the band in ^{156}Dy . The multivalued dependence in the region around $\omega = 0.3 \text{ MeV}/\hbar$ corresponds to the crossing between the two orbitals (i.e. two Routhian curves cross at certain ω_{cross}) lying on the yrast line. Since ω is determined as a slope in the curve of energy E as function of I (cf. eq. (8)) the kinematical moment of inertia $\mathcal{J}^{(1)}$ undergoes a sharp change (with $\Delta\omega < 0$ locally) bending back in the plane of $\mathcal{J}^{(1)}$ versus ω . This behaviour is often referred to as backbending [9]. The dynamical moment of inertia $\mathcal{J}^{(2)}$ exhibits even more rapid changes at the crossing point. If the crossing were ideally sharp the derivative $dI/d\omega$ would become singular with a jump from $+\infty$ down to $-\infty$. This is illustrated in Fig. 1.2b). Generally speaking all the configurations allowing for a rapid alignment in angular momentum give a large, positive contribution to $\mathcal{J}^{(2)}$ according to eq. (13). On the other hand, if at certain region the nuclear configurations have a structure of closed shells, or subshells (or, in other words, there are no more orbits around the Fermi surface carrying large changes in $\langle \mathcal{J}_1 \rangle$) then the angular momentum does not increase fast enough with ω and, consequently, the quantity $\mathcal{J}^{(2)}$ decreases in this region. Let us compare for example the superdeformed bands in the two neighbouring nuclei ^{152}Dy and ^{150}Gd (see Fig. 1.3). The $\mathcal{J}^{(2)}$ moment of inertia in ^{152}Dy is roughly constant while in ^{150}Gd a rapid decrease in $\mathcal{J}^{(2)}$ versus ω can be seen. Fig. 1.3b) illustrates the orbit occupation of Routhians by protons. One can see that in ^{150}Gd where the 64 protons are occupied a rather wide gap appears so that no more aligned orbits can be found below the Fermi surface. This situation is contrasted with ^{152}Dy where the occupation of the 651 3/2 orbit leads to a rapid increase in the aligned angular momentum thus restoring the constant value of $\mathcal{J}^{(2)}$.

We shall only briefly mention two other phenomena that can occur in the domain of fast rotation: the band termination and the noncollective rotation. If the prolate nucleus which is originally axially symmetric (say, with respect to the x'_3 -axis) rotates

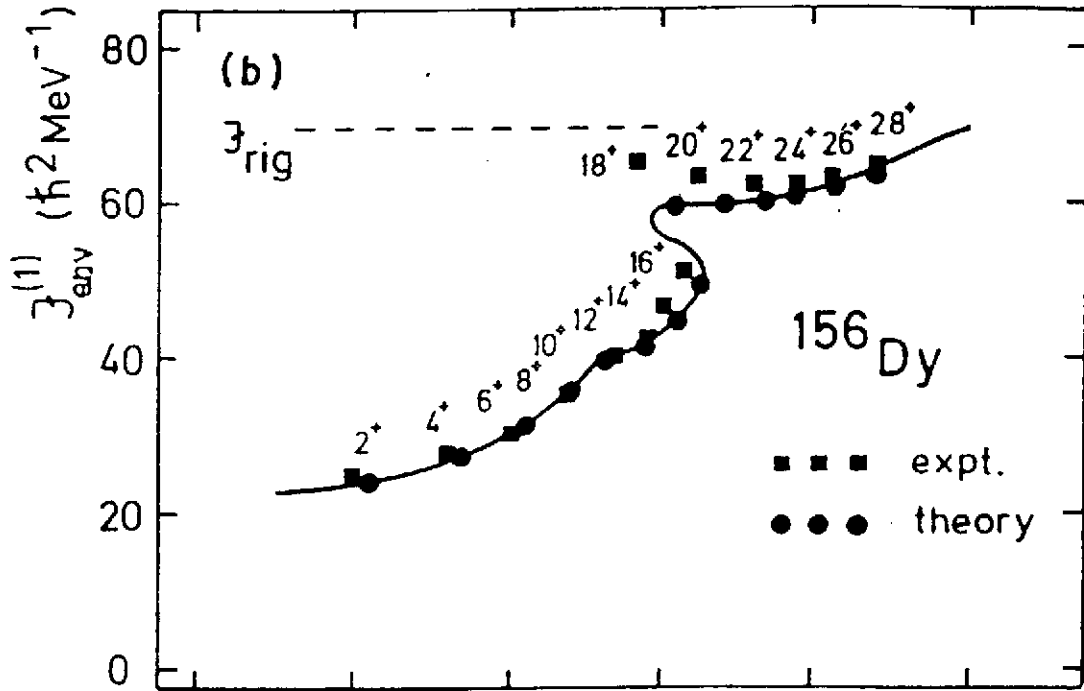


Fig. 1.2a

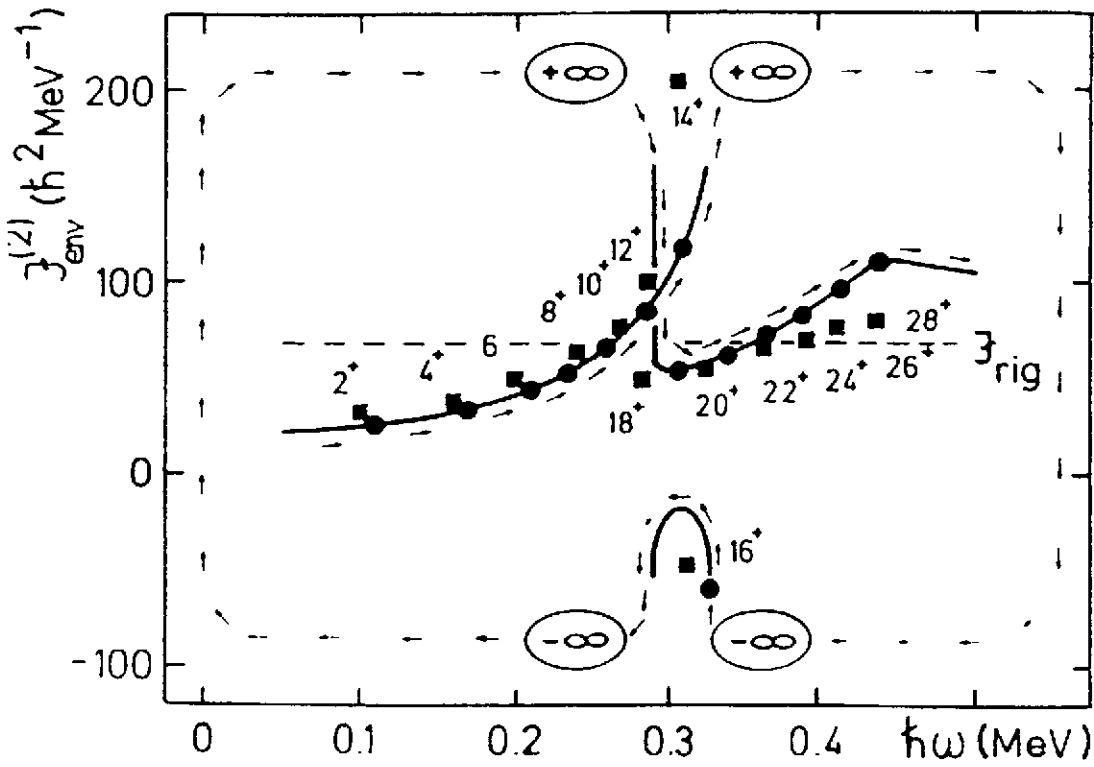


Fig. 1.2b

Fig. 1.3a

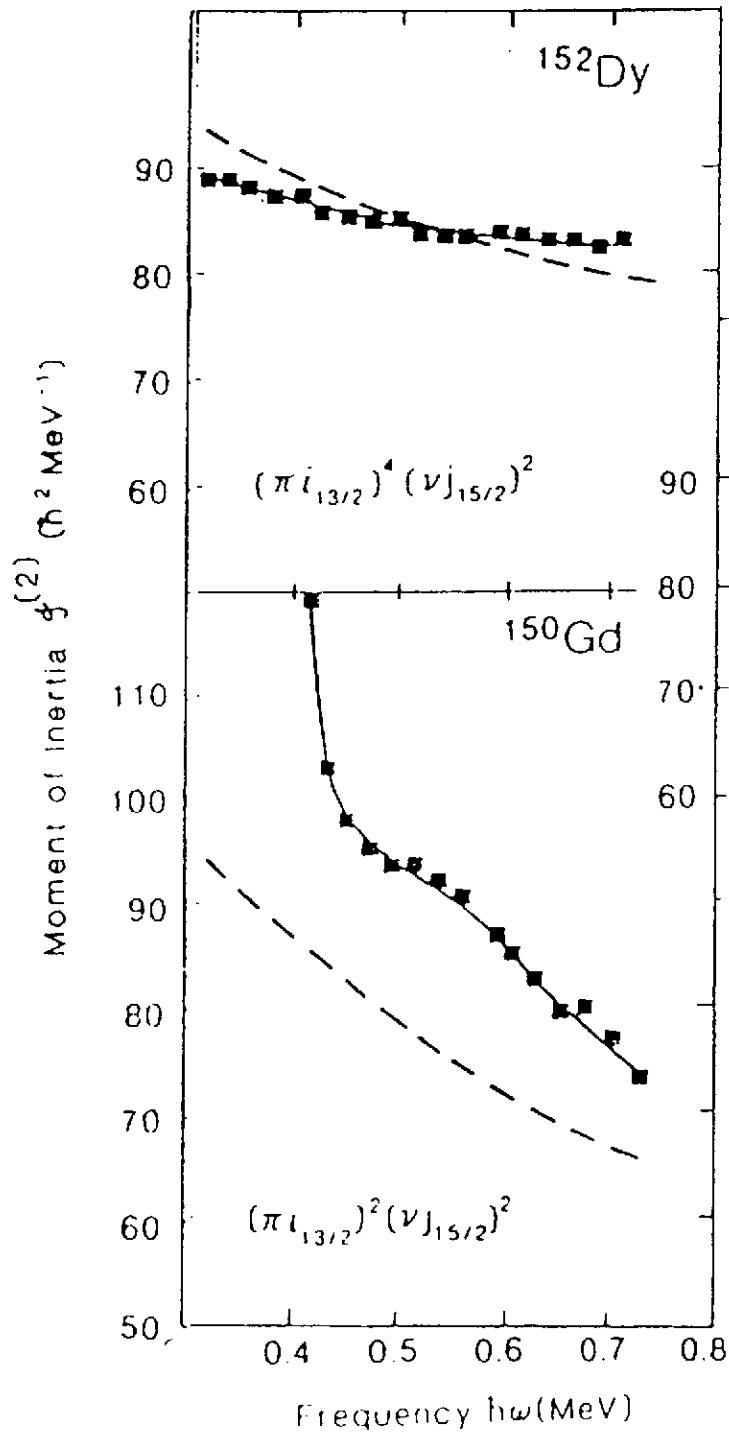
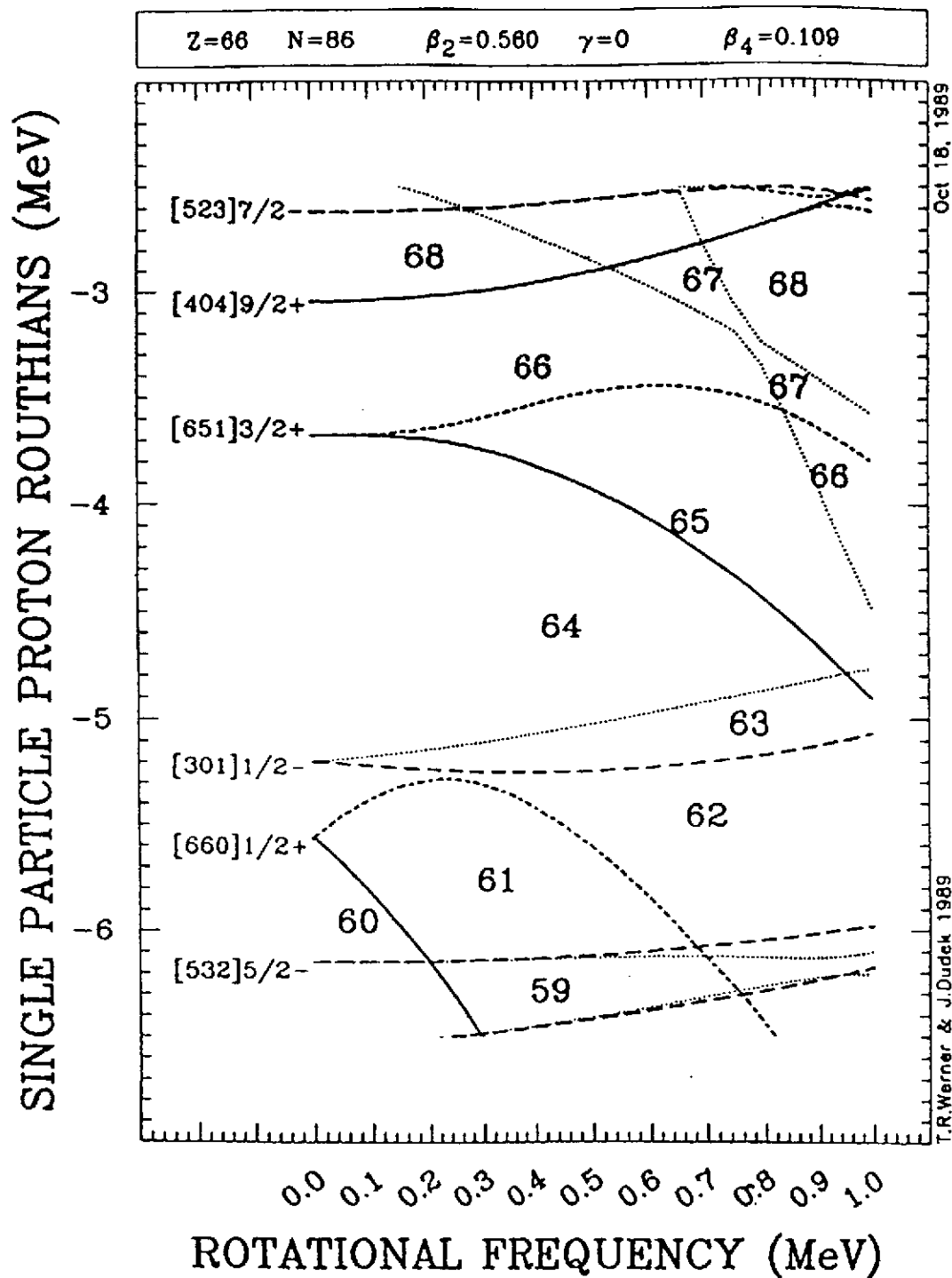


Fig. 1.3b



faster and faster about an axis perpendicular to the x'_3 -axis (say, the $x_1 = x'_1$ -axis) it may exhibit a tendency of adjusting its shape by attempting to locate more and more of its mass in the $x'_2x'_3$ -plane. The resulting limiting value (band termination) occurs when the shape of the nucleus becomes axially symmetric (and generally oblate) with respect to the x'_1 -axis (i.e. the rotation axis). Further collective rotation is no more possible. Further increase in the angular momentum above the point of band termination is only possible when the nucleonic configuration change. This single-particle mechanism of gaining angular momentum has, therefore, a less regular character corresponding to its single-particle structure. In particular, some isomeric states ("yrast traps") are possible in this region. We shall not deal with the last two phenomena as they seem to be irrelevant in the region of very much deformed nuclei that rotate fast (i.e. in the region of superdeformation).

2 Shell Structure

In order to discuss the possible onset of the very large deformations in nuclei induced by a fast rotation it is instructive to consider first the behaviour of an average nuclear system (i.e. independent of the detailed nucleonic configurations and their quantal structure). We shall thus consider first a rotation in the framework of classical physics and introduce a finite portion of nuclear matter which is able to respond to rotation mostly by changing its shape [11]. The centrifugal forces tend to deform the nucleus by locating as much mass as possible far from the rotation axis and compete with surface tension attempting to restore spherical shape. In addition, the tendency of deforming the nucleus is helped by the Coulomb repulsion between the protons. As a result of these tendencies the nucleus which is spherical at $I = 0$ becomes oblate deformed and increases its deformation in the region of I between $I = 0$ and $I = I_{crit}$. At certain critical value I_{crit} of angular momentum the system with oblate shape becomes unstable in favor of triaxial distortions tending finally (with further increase of I) to the very elongated (prolate) shapes. This point can be considered as a transition to the superdeformed shape of an average nucleus described in terms of a rotating liquid drop. Some details of the above approach have been described in a lecture presented couple of years ago at this School [12]. The transition described above is well known in hydrodynamics as the Jacobi instability and was commonly applied in the investigations of the shapes in the rotating astronomical objects such as stars, planets, asteroids etc. (for some comparisons with nuclei see e.g. the reviews [12] and [13]). The astronomical objects are known to be oblate deformed in the

Table 2.1

=====

Typical Deformations.

Planets	β	Nuclei (A)	β
Mercury	0.0	(20)Ne	0.55
Venus	0.0	(156)Gd	0.25
Earth	-0.0036	(160)Dy	0.26
Moon	-0.0021	(170)Yb	0.28
Mars	-0.0062	(232)Th	0.20
Jupiter	-0.0671	(238)U	0.22
Saturn	-0.107	(244)Pu	0.23
Uranus	-0.025	(260)Fm	0.23
Pluto	?		

(some triaxial shapes):

Satelites	(km)	Nuclei	(fm)
(Martian)			
Phobos	27x21.4x19.2	(24)Mg	4.64 3.33x2.67
Deimos	15x12x11		
(Jovian)			
Amalthea	135x85x77		
Asteroids			
Metis	122x95x55		
Kalliope	108x80x65		
Laetitia	128x75x42		

domain of a slow rotation. The existence of double stars may be considered as a result of fission following the formation of large elongated shapes due to the Jacobi instability. Some examples of comparison between the astronomical objects and nuclei are illustrated in Table 2.1 (taken from ref. [13]).

This beautiful analogy between stars, planets etc. from one side and atomic nuclei from the other should not perhaps be pushed too far. The main difference between the two physical systems lies in the obviously quantal structure of the physical laws governing atomic nuclei while astronomical objects remain classical.

It appears that the bunching in the quantal energy levels into shells has an important effect on nuclear structure and can modify essentially the response of the nuclear system to a fast rotation. Indeed it is the density of quantal levels near the Fermi surface, or — more generally — near the yrast line that is crucial for the argument. If the number of nucleons in a given nucleus corresponds at certain deformation to the very low local density of levels the system is relatively more stable and the formation of the exotic state (like the superdeformed one) becomes possible. In the situation of the extreme bunching of levels the corresponding numbers of nucleons may be considered as magic ones which are especially favourable for the formation of stable (or relatively more stable as compared to its neighbourhood) exotic states. Let us study this effect in a simplest system of independent nucleons in a potential of a nonrotating three dimensional anisotropic h.o. (=harmonic oscillator). It appears that even at the highest angular momenta seen in experiments so far the resulting rotational frequency ω is in most cases appreciably lower than the frequencies ω_1 , ω_2 and ω_3 characterising the h.o. potential. Thus in the first rough approximation we can disregard entirely the effect of rotation on the shell structure. The single-particle energies of a nucleon

$$e_{n_1 n_2 n_3} = \hbar\omega_1(n_1 + 1/2) + \hbar\omega_2(n_2 + 1/2) + \hbar\omega_3(n_3 + 1/2) \quad (16)$$

are characterised by the three frequencies ω_i and three quantum numbers n_i , ($i = 1, 2, 3$). One may employ the Nilsson deformation parameters ϵ and γ and express the three h.o. frequencies as

$$\begin{aligned} \omega_1 &= \omega_0(\epsilon, \gamma) \left\{ 1 + (1/3)\epsilon \cos \gamma + (\epsilon/\sqrt{3}) \sin \gamma \right\} \\ \omega_2 &= \omega_0(\epsilon, \gamma) \left\{ 1 + (1/3)\epsilon \cos \gamma - (\epsilon/\sqrt{3}) \sin \gamma \right\} \\ \omega_3 &= \omega_0(\epsilon, \gamma) \left\{ 1 - (2/3)\epsilon \cos \gamma \right\} \end{aligned} \quad (17)$$

where the dependence of ω_0 on ϵ and γ follows from the volume conservation condition

$$\omega_1 \omega_2 \omega_3 = \omega_0^3 \quad (18)$$

with ω_0 being a constant independent of ϵ and γ .

The Bohr and Mottelson condition (ref. [4]) for the existence of the shell structure leads in this case to the requirement that the three h.o. frequencies ω_i are proportional to the three (generally not very large) integer numbers

$$\omega_1 : \omega_2 : \omega_3 = a : b : c \quad (19)$$

It is very easy to see that the single-particle states with the same value of the quantum number N_{shell} defined as (ref. [4])

$$N_{shell} = an_1 + bn_2 + cn_3 \quad (20)$$

have the same energy. Thus the quantum number N_{shell} determines a set of degenerate states i.e.a shell for the deformation specified by eq. (19). Obviously further symmetries of the system are able to increase the degeneracy in the shell and, therefore, to make the bunching of levels even more pronounced. Thus in the case of spherical symmetry, $a = b = c = 1$ the harmonic oscillator becomes isotropic and the quantum number N_{shell} overlaps with the main h.o. quantum number N :

$$N_{shell} = N = n_1 + n_2 + n_3 \quad (21)$$

The corresponding magic numbers define the closed shells with number of nucleons 2, 8, 20, 40, ...

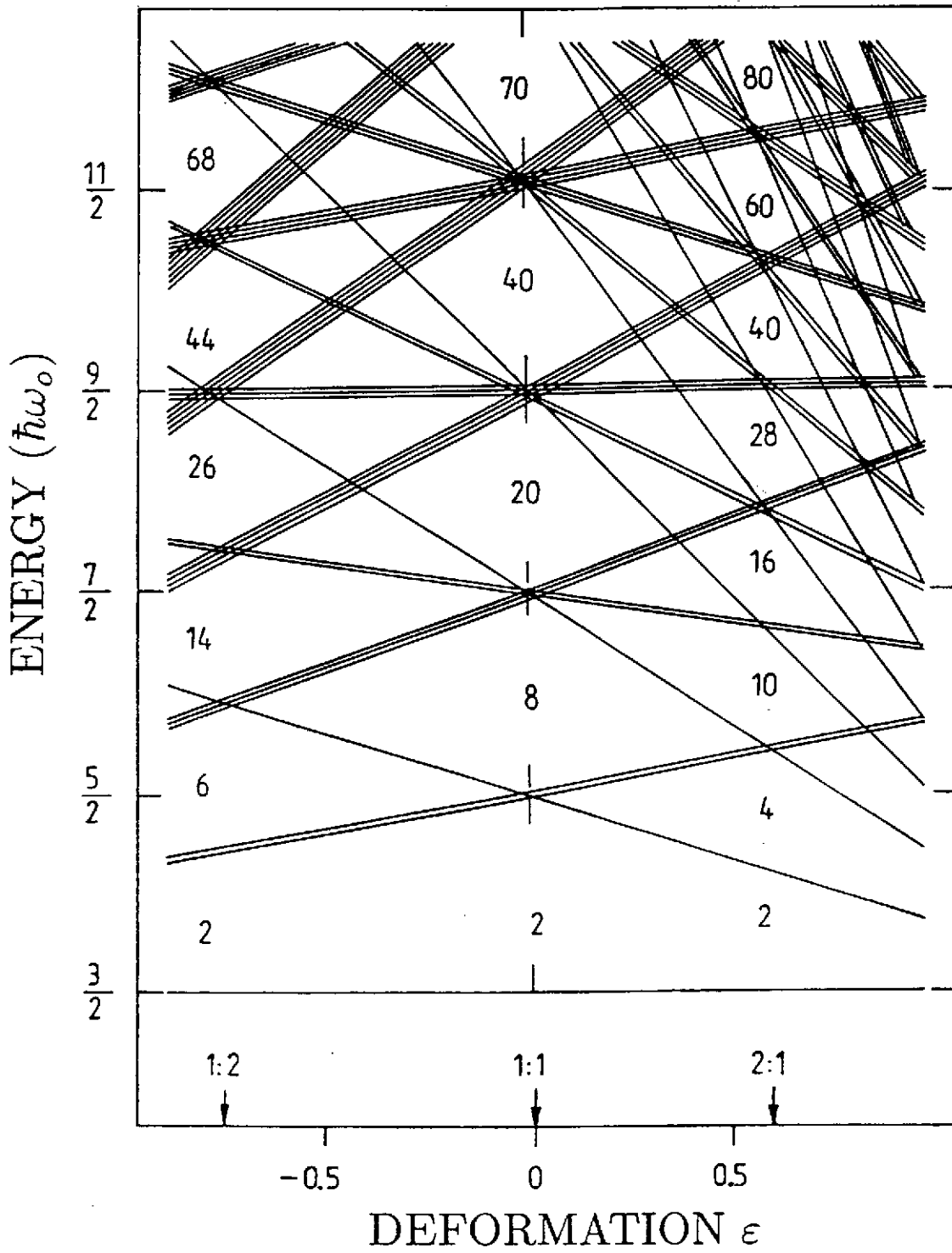
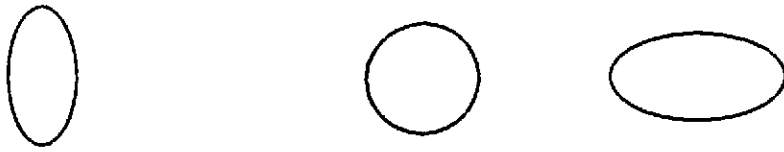
The case of axial symmetry leads also to some simplifications although the corresponding shell structure exhibits less degeneracies than in the isotropic case. Here, we can distinguish two possible chains of shapes with different shell structures, the prolate ones with

$$\begin{aligned} (a, b, c) &= (2, 2, 1) && \text{(superdeformed)} \\ &= (3, 3, 1) && \text{(hyperdeformed)} \\ &\dots && \text{(etc.)} \end{aligned}$$

and the oblate ones

$$\begin{aligned} (a, b, c) &= (1, 1, 2) && \text{(we may call it superoblate)} \\ &= (1, 1, 3) && \text{(we may call it hyperoblate)} \\ &\dots && \text{(etc.)} \end{aligned}$$

Fig. 2.1



The series of magic numbers corresponding to the closed (deformed) shells determined by the sets of numbers (a, b, c) are:

$$\begin{aligned} 2, 4, 10, 16, \dots & \text{ (superdeformed)} \\ 2, 4, 6, 12, \dots & \text{ (hiperdeformed)} \end{aligned}$$

and

$$\begin{aligned} 2, 6, 14, 26, \dots & \text{ (superoblate)} \\ 2, 6, 12, 22, \dots & \text{ (hiperoblate)} \\ \dots\dots\dots & \text{ (etc.)} \end{aligned}$$

Fig. 2.1 illustrates the h.o. levels plotted versus ϵ for the axially symmetric shapes ($\gamma = 0^\circ$ or 60°). The spherical, superdeformed and superoblate shells can be easily identified.

Let us now investigate some of the possible triaxial cases leading also to some shell structure. In these cases, however, the shell effects become relatively weaker as there is less symmetry in the configurations leading to the less degenerate shells. Some configurations that seem to be simplest in this case may be called supertriaxial ($\omega_1 : \omega_2 : \omega_3 = 4 : 3 : 2$), hipertriaxial ($3 : 2 : 1$) etc. They define magic numbers as

$$\begin{aligned} 2, 2, 4, 6, 10, \dots & \text{ (supertraxial)} \\ 2, 4, 8, 14, 20, \dots & \text{ (hipertriaxial)} \\ \dots\dots\dots & \text{ (etc.)} \end{aligned}$$

Table 2.2 summarises all the deformed shells in the anisotropic harmonic oscillator which were discussed above.

All the possibilities for the formation of the exotic states presented so far correspond to the ideal case of the nuclear potential of a harmonic oscillator. In order to search for the more realistic description more refined potentials such as those of the modified h.o. (Nilsson), Woods-Saxon, folded Yukawa etc. (if not even more basic potentials generated by the Hartree-Fock procedure) should be employed. Some calculations in this direction have already been started (cf. refs. [14],[15]). We shall not go into detailed descriptions of these investigations. Instead, we would like to consider briefly a possibility of a simplified treatment that follows from the introduction of a specific symmetry in the nuclear systems, namely the pseudospin and pseudo-SU(3) symmetries. The natural symmetry related to the pure harmonic oscillator is as well

Table 2.2.

=====

Shell Structure in The Anisotropic Harmonic Oscillator.

	a:b:c	ϵ	γ	Magic numbers
spherical	1:1:1	0.0	0°	2, 8, 20, 40, 70, 112, 156, ...
superdeformed	2:2:1	0.600	0°	2, 4, 10, 16, 28, 40, 60, ...
hyperdeformed	3:3:1	0.657	0°	2, 4, 6, 12, 18, 24, 36, 48, 60, ...
.....
superoblate	1:1:2	0.750	60°	2, 6, 14, 26, 44, 68, 100, ...
hyperoblate	1:1:3	1.200	60°	2, 6, 12, 22, 36, 54, 78, 108, ...
.....
supertriaxial	4:3:2	0.577	30°	2, 4, 6, 10, 12, 18, 22, 30, 36, 46, 54, ...
hypertriaxial	3:2:1	0.839	30°	2, 4, 8, 14, 20, 30, 44, ...
.....

known, the special unitary symmetry in three dimensions i.e. the $SU(3)$ symmetry [16]. However, the main failure of the pure h.o. nuclear potential consists on the lack of possibility of including the strong $\vec{l} \cdot \vec{s}$ coupling in the nuclear Hamiltonian. Indeed, the $\vec{l} \cdot \vec{s}$ term in the nucleus is strong enough to be able to shift from an every N -shell one subshell of highest orbital angular momentum $l = N$ and total angular momentum $j = l + 1/2$ down to the lower shell. Thus for example the $j_{15/2}$, $i_{13/2}$, $h_{11/2}$, etc. orbitals are shifted down from $N = 7$ to $N = 6$, from $N = 6$ to $N = 5$, from $N = 5$ to $N = 4$ etc., respectively. These are the well-known intruder states.

If for the moment we take apart the intruder states from each shell the remaining states in each major h.o. shell N (the so called normal parity states) may be cast artificially into a new major h.o. shell \tilde{N} with $\tilde{N} = N - 1$. All the states $|Nljm\rangle$ except the intruder states can thus be renamed as the states of $|\tilde{N}\tilde{l}\tilde{j}\tilde{m}\rangle$ with the following rule

$$|Nljm\rangle \Rightarrow |\tilde{N}\tilde{l}\tilde{j}\tilde{m}\rangle$$

with

$$\begin{aligned} \tilde{N} &= N - 1 \\ \tilde{l} &= l \pm 1 \text{ (for } j = l \pm 1/2) \\ \tilde{j} &= j \\ \tilde{m} &= m \end{aligned} \quad (22)$$

This artificial procedure proves to be fruitful in that sense that all the normal parity states can then be described by the $\widetilde{SU}(3)$ (pseudo- $SU(3)$) which is nothing else as the usual $SU(3)$ symmetry related to the renamed \tilde{N} shell (cf. refs. [17],[18]). On the other hand, the intruder states have to be added finally as other states that do not belong to the $\widetilde{SU}(3)$ scheme. Following the above procedure one can thus plot the nuclear energy levels as functions of deformation ϵ by employing the harmonic oscillator scheme for all the \tilde{N} -shells and finally add all the intruder states that have been originally removed from the picture [19]. Fig.2.2 has been constructed by following the above recipe. The levels shown correspond to one type of nucleons (neutrons or protons, separately). Resulting "magic" numbers of nucleons i.e. the regions of low density of levels can be read off from this picture. It can be seen that the magic numbers corresponding to the deformation range $\epsilon \sim 0.4$ to 0.7 occur around nucleon numbers in the regions 28-32, 38-46, 58-66, 72-86 and finally 100-114. This explains very well the existence of the superdeformed shape in ^{152}Dy with $\epsilon \approx 0.6$, $Z = 66$ and $N = 86$. Similar features show up for $Z = 80$ and $N = 112$ i.e. around the nucleus ^{192}Hg .

3 Symmetries

In this section we shall discuss some properties of the superdeformed rotational bands in nuclei having in mind mostly the $A = 150$ region (i.e. roughly around $Z \sim 66$ and $N \sim 86$). The region around $A = 190$ (with $Z \sim 80$ and $N \sim 110$) exhibits similar features.

One of the most striking phenomenon is the appearance of the identical bands in the superdeformed region in some neighbouring pairs of nuclei. The identity means that the gamma-ray energies $E_{\gamma I}$ in one nucleus are equal to a very good approximation to the gamma-ray energies $E'_{\gamma I'}$ in the other nucleus. Two examples of such pairs of bands are shown in Table 3.1. The pairs of identical bands are also called twin bands. The almost exact (sometimes up to a fraction of 1 keV!) overlap of the gamma-ray energies coming from neighbouring nuclei is intriguing since in general the properties of neighbouring nuclei are never similar within a precision of 1keV.

Apart from the indential bands some other relations between the gamma-ray energies $E_{\gamma I}$ in neighbouring nuclei have been observed. In some pairs for instance the quantities $E_{\gamma I}$ appear to be equal to a good approximation to the arithmetic averages of the energies in the neighbouring nucleus: $1/2(E'_{\gamma I'} + E'_{\gamma I'+2})$. This relation is sometimes referred to as the indirect twin bands. Finally, some different type of (weighted) averages hold in corresponding pairs $E_{\gamma I} = 3/4E'_{\gamma I'} + 1/4E'_{\gamma I'+2}$ (called coupled pairs). The analysis of the above relations will be the topic of our main interest in this section.

Since the phenomena mentioned above seem to be related with the pseudo- $SU(3)$ and pseudospin symmetries let us first recall the most essential features of these symmetries (cf refs. [17] and [18]). Without following the historical path in the development of the concepts of those symmetries let us start by considering the recipes for changing the labels of the usual shell-model independent-particle states into the notation of the pseudo- $SU(3)$ (i.e. $\widetilde{SU}(3)$) scheme. The relabelling of the states $|Nljm\rangle$ in a spherical potential has been already specified before (cf.eq. (22)).

Now, the degeneracy of all the states $|\widetilde{N}\widetilde{l}\widetilde{j}\widetilde{m}\rangle$ with respect to the quantum numbers $\widetilde{l}, \widetilde{j}$ and \widetilde{m} (but not \widetilde{N}) is just equivalent to the assumption of the pseudo- $SU(3)$ symmetry. Obviously, the pseudo- $SU(3)$ symmetry is only a crude approximation. A less restrictive symmetry is provided by the pseudospin symmetry that requires only the degeneracy between the pairs of states $|\widetilde{N}\widetilde{l}\widetilde{j}\widetilde{m}\rangle$ with respect to $\widetilde{j} = \widetilde{l} \pm (1/2)$ (apart, of course, from the standard degeneracy with respect to \widetilde{m}). Thus for example within the pseudospin symmetry the pairs of states $(g_{7/2}, d_{5/2})$ in other notation $(\widetilde{f}_{7/2}, \widetilde{f}_{5/2})$

Table 3.1

=====

Examples of Identical Bands.
 (experimental gamma-ray energies in keV)

150 Gd(II)	151 Tb(I)	151 Tb(II)	152 Dy
	1432.5	1449.0	1449.4
1378.0	1380.7	1401.2	1401.7
1327.0	1330.0	1354.0	1353.0
1277.0	1278.5	1305.0	1304.7
1228.0	1228.5	1255.0	1256.0
1179.0	1179.9	1207.0	1208.7
1131.0	1130.2	1160.8	1160.8
1084.0	1082.5	1111.9	1112.7
1037.0	1034.9	1064.0	1064.8
991.0	983.7	1016.0	1017.0
944.0	942.8	969.4	970.0
901.0	898.0	923.1	923.1
857.0	854.0	875.6	876.1
813.0	811.3	829.3	829.2
771.0	769.2	783.0	783.5
	728.0	736.8	737.5
		691.9	692.2
		646.9	647.2
		602.3	602.3

are degenerate. The same holds for a pair $(d_{3/2}, s_{1/2}) = (\widetilde{p}_{3/2}, \widetilde{p}_{1/2})$ etc. In the more restrictive case of an $SU(3)$ symmetry all the above four states (belonging to $N = 4$ i.e. $\tilde{N} = 3$) are degenerate. Of course the last symmetry is valid only very approximately in nuclei.

Now, it turns out that the $SU(3)$ symmetry can be approximately extended into the deformed potentials. Namely the standard Nilsson asymptotic representation $|Nn_3\Lambda l\rangle$ transforms as

$$|Nn_3\Lambda\Omega\rangle \implies |\tilde{N}\tilde{n}_3\tilde{\Lambda}\tilde{\Omega}\rangle$$

with

$$\begin{aligned} \tilde{N} &= N - 1 \\ \tilde{n}_3 &= n_3 \\ \tilde{\Lambda} &= \Lambda \pm 1 \text{ (for } \Omega = \Lambda \pm 1/2) \\ \tilde{\Omega} &= \Omega \end{aligned} \tag{23}$$

Thus for example some of the $N = 5$ ($\tilde{N} = 4$) states transform as

$$\begin{aligned} 541 \ 1/2 &\longrightarrow 440 \widetilde{1/2} \\ 530 \ 1/2 &\longrightarrow 431 \widetilde{1/2} \\ 532 \ 3/2 &\longrightarrow 431 \widetilde{3/2} \\ 521 \ 3/2 &\longrightarrow 422 \widetilde{3/2} \quad \text{etc.} \end{aligned} \tag{24}$$

On the other hand, the intruder $N = 5$ states: 550 1/2, 541 3/2, 532 5/2, 523 7/2, 514 9/2 and 505 11/2 have no corresponding partners in the pseudospin scheme.

Let us now see what are the quantal orbits filling in one degenerate shell in the case of a superdeformed potential ($\epsilon = 0.6; \gamma = 0^\circ$) in a pseudo- $SU(3)$ representation. Let us choose for example all the states that fill in the degenerate shell just above 66 nucleons in Fig. 2.2. It is easy to see that all these states form a 2:2:1 shell characterised by the quantum number

$$\tilde{N}_{shell} = 2\tilde{n}_\perp + \tilde{n}_3 = 5 \tag{25}$$

(the tildas over all the symbols in the above equation are to remind us that we are dealing with the $\widetilde{SU}(3)$ scheme instead of $SU(3)$). It is also easy to see that these states come from three pseudo-h.o. major shells with $N = 3, 4$ and 5. Labelling those states with quantum numbers $(\tilde{n}_3, \tilde{n}_\perp, \tilde{\Lambda})$ which are defined as a

product of states $|\tilde{n}_3\rangle$ of a one-dimensional h.o. along the third axis with states $|n_{\perp}\tilde{\Lambda}\rangle$ of a two-dimensional h.o. in the $(x'_1x'_2)$ plane we obtain the following set of states in the superdeformed shell characterised by $\tilde{N}_{shell} = 5$ (cf. eq. (25)):

$$\begin{array}{ccccc} & & (5, 0, 0) & & \\ & & (3, 1, -1) & & (3, 1, 1) \\ (1, 2, -2) & & (1, 2, 0) & & (1, 2, 1) \end{array}$$

Including in addition the spin degeneracy $(+1/2)$ we obtain altogether 12 states in this shell which are strictly degenerate for the pure pseudo- $SU(3)$ scheme and should lie close to each other if the pseudo- $SU(3)$ symmetry is a good approximation.

Let us now see how the existence of the identical bands can be described in terms of the particle-rotor model [21] when the odd- A nucleus exhibits a $K = 1/2$ band. Thus modified expression (3) rather than (1) should be applied. It appears that the decoupling parameter a can be calculated in a closed form in the case of a pure h.o. potential. The result is

$$a = (-1)^N \tag{26}$$

where N is the major h.o. quantum number. In the case of a pseudo- $SU(3)$ symmetry the argument goes in analogous way except that N should be replaced by $\tilde{N} = N - 1$. Thus in the case of a pseudo- $SU(3)$ symmetry the decoupling parameter a is equal to

$$a = (-1)^{\tilde{N}} = -(-1)^N \tag{27}$$

Now it follows from eq. (1) that the gamma-ray energies are

$$E_{\gamma I} = E_{I+2} - E_I = \frac{\hbar^2}{2\mathcal{J}}(4I + 6) \tag{28}$$

On the other hand, the gamma-ray energies in the neighbouring odd nucleus with $K = 1/2$ have to be calculated from eq. (3)

$$E'_{\gamma I'} = \frac{\hbar^2}{2\mathcal{J}'} \{4I' + 6 + 2a(-1)^{I'+1/2}\} \tag{29}$$

Let us now assume that

$$\begin{array}{l} \mathcal{J}' = \mathcal{J} \\ a = +1 \\ I' = I + 1/2 \end{array} \tag{30}$$

In this case we obtain the relation

$$E_{\gamma I} = E'_{\gamma I'} \quad (31)$$

which is just the relation characterising the twin bands. On the other hand, if $a = -1$ the bands are not identical but instead

$$E'_{\gamma I'} = 1/2(E_{\gamma I} + E_{\gamma I+2}) \quad (32)$$

as can be easily seen from eq. (29). The two bands are then the indirect twin bands. Finally, if the odd- A band is characterised by $K \neq 1/2$ we have $a = 0$ and one has to apply formula (1) for both the bands in the even and odd- A nuclei. In this case it is easy to deduce (all the time we assume $\mathcal{J}' = \mathcal{J}$ and $I' = I + 1/2$) that

$$E'_{\gamma I'} = 3/4 E_{\gamma I} + 1/4 E_{\gamma I+2} \quad (33)$$

This is just the case of coupled bands. One has to emphasize that relations (31), (32) and (33) are only special cases and in general no definite relations between the neighbouring bands can be observed. All the above considerations have been deduced in the framework of the particle-rotor model.

Another description of the relations between the superdeformed rotational bands discussed above can be provided in terms of the angular momentum alignment ([22],[23]) of one rotational band (say, in the odd- A nucleus) relative to the neighbouring band (say, in the even nucleus). Suppose that the dynamical moment of inertia $\mathcal{J}^{(2)}$ in a band is constant. Then the plot of angular momentum versus the gamma-ray energies $E_{\gamma I}$ is a straight line

$$I = m E_{\gamma I} + b \quad (34)$$

where parameter m is proportional to the moment of inertia $\mathcal{J}^{(2)}$ and parameter b is related to the alignment. It is generally agreed by the experimentalists that the consecutive gamma-ray energies $E_{\gamma I}$ correspond to I changing in intervals of 2, i.e. form a series

$$E_{\gamma I}, E_{\gamma I+2}, E_{\gamma I+4}, \dots$$

Then taking two values differing by $\Delta I = 2$ we obtain

$$m = \frac{2}{E_{\gamma I+2} - E_{\gamma I}} \quad (35)$$

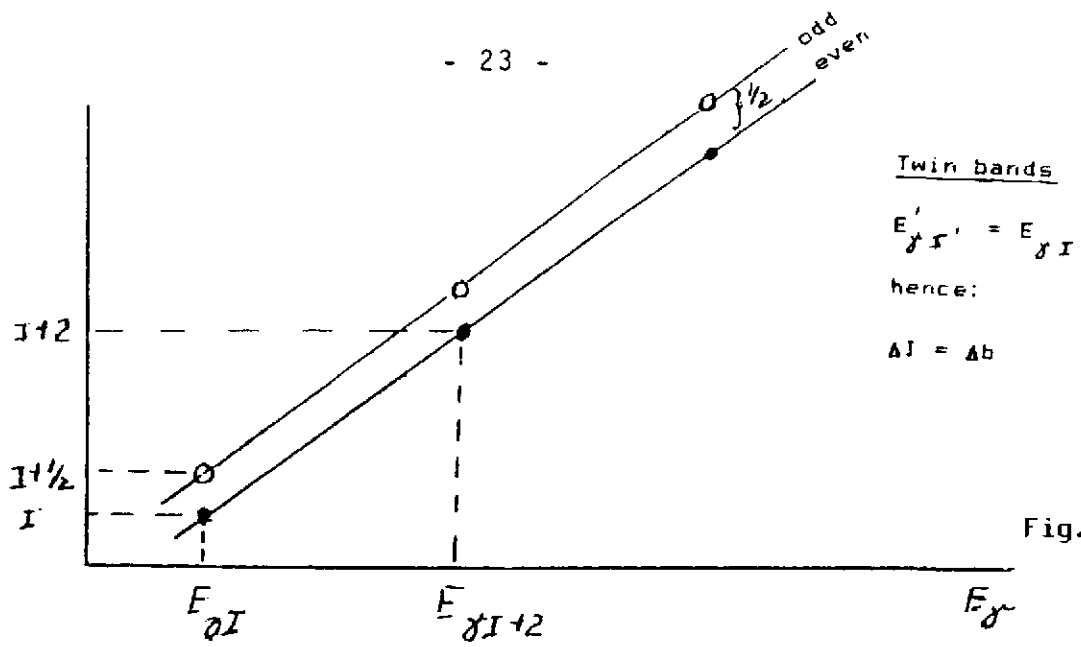


Fig. 3.1a

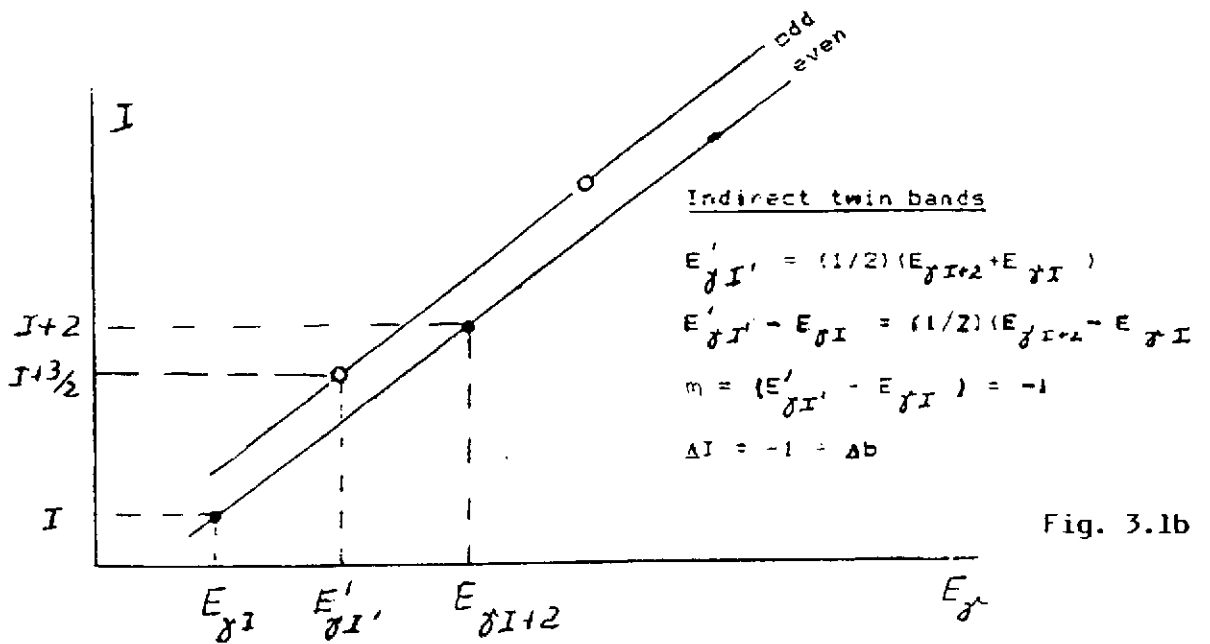


Fig. 3.1b

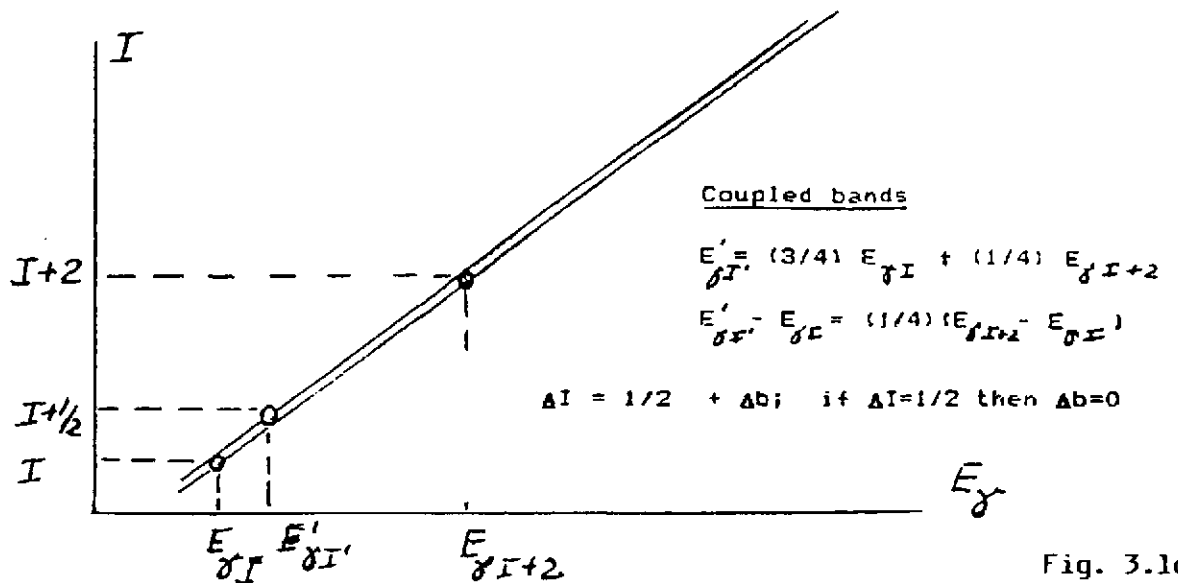


Fig. 3.1c

In the neighbouring (say, odd- A) nucleus we may expect a relation similar to that given by eq. (34) (say, valid for an even nucleus)

$$I' = mE'_{\gamma I'} + b' \quad (36)$$

where we have assumed the same moment of inertia in both the bands ($m = m'$). Substraction (36) minus (34) gives

$$\Delta I = \{m(E'_{\gamma I'} - E_{\gamma I}) + \Delta b\} \text{ mod } 2 \quad (37)$$

The term mod 2 in this formula comes from the fact that $I - I'$ is known only up to an integer multiple of 2. Here:

$$\Delta I = I' - I$$

and

$$\Delta b = b' - b$$

Eq. (37) may now be applied to the three possible cases: the twin bands, indirect twin bands and coupled bands (cf. eqs. (31), (32) and (33), respectively). The results are

$$\Delta I = \Delta b \text{ mod } 2 \quad (38)$$

for the twin bands,

$$\Delta I = (1 + \Delta b) \text{ mod } 2 \quad (39)$$

for the indirect twin bands and finally

$$\Delta I = (1/2 + \Delta b) \text{ mod } 2 \quad (40)$$

for the coupled bands. Last equation implies that $\Delta b = 0$ if ΔI were known to be $\Delta I = 1/2$. The above three possibilities are illustrated in Fig. 3.1a,b,c). Let us observe that the above considerations lead to the conclusion that in all the three above cases the alignment is quantised which seems to be an intriguing result since angular momentum projection on the x'_1 -axis is defined as an expectation value only and thus should not be quantised in principle.

Finally, let us observe that the relative alignment between the two bands (36) and (34) can be also estimated from the theory employing the single-particle Routhians e_{ν}^{ω} as known functions of rotational frequency ω . Indeed according to eq. (9) the slope in the Routhian curve (taken with minus sign) denotes its individual contribution

to the alignment. Thus the valence orbit in the odd-nucleus should have individual alignments

$$(j_1)_{\nu\nu} = -\frac{\partial e_{\nu}^{\omega}}{\partial \omega} \quad (41)$$

Let us observe that some definite relations for the alignment follow from the $\widetilde{SU}(3)$ symmetry in the superdeformed bands (cf. refs. [22] and [23]). Indeed, considering an example of the $N_{shell} = 5$ shell (cf. eq. (25) and the following text) we can conclude that the orbital part of angular momentum \tilde{l}_1 cannot couple the states within one N_{shell} . In fact, \tilde{l}_1 can only couple states with $\Delta n_3 = +1$ while the states forming one shell contain only those values of n_3 that differ by two units: $\Delta n_3 = 0, 2, 4, \dots$. Thus in the cranking Hamiltonian

$$H^{\omega} = H - \hbar\omega\tilde{j}_1 = H - \hbar\omega\tilde{l}_1 - \hbar\omega\tilde{s}_1 \quad (42)$$

only the spin part \tilde{s}_1 can be active within a shell and, consequently, the resulting alignment can be only $\pm 1/2$. Thus in principle all the Routhian plots within the normal parity states in a superdeformed region should have the slopes ($\frac{\partial e_{\nu}^{\omega}}{\partial \omega}$) equal $-1/2$ or $+1/2$. This justifies the argument for the existence of the twin-, or indirect twin-bands. The above arguments are, however, only approximate since first of all the $SU(3)$ symmetry does not hold exactly and second, there exists always a certain interaction with the intruder states which do not obey the above restrictions.

As a last topic in this section let us describe attempts to understand the phenomenon of twin bands, indirect twin bands etc. in terms of nuclear structure. The considerations discussed above give only the description of the phenomena either in terms of the decoupling parameter or else the relative alignment without really explaining why the moments of inertia in the two neighbouring bands are almost equal. Before presenting an attempt to answer this question let us see once again why this phenomenon seems to be so strange. In fact, when we add one nucleon to the rotating core several effects are expected. First of all the change in nuclear radius is expected and this should increase the moment of inertia. Simple estimates indicate that this fact should cause a change in the gamma-ray energies by an amount of the order of 10 keV i.e. one order of magnitude more than the observed differences in the twin bands. Similar effects are expected due to the polarisation of the nuclear core induced by the presence of one additional nucleon. Finally, nuclear rotation causes the alignment in nucleonic orbits which can also a priori cause differences between the even and odd- A systems.

Let us now see how one can attempt to estimate some of the effects mentioned above [24],[25]. If the pseudo- $SU(3)$ is a good symmetry in the nucleus at high angular

momentum then the normal parity states in the nucleus should resemble roughly those in the harmonic oscillator. Let us first neglect the nuclear rotation. This approximation should be not so bad since even at the states with angular momentum considered as very high the corresponding angular velocity is still appreciably small as compared to the h.o. frequencies. Thus let us employ [25] an expression for the nuclear moment of inertia \mathcal{J} calculated in the nonrotating h.o. potential. The corresponding formula was obtained long ago by A. Bohr and B. R. Mottelson [26]

$$\mathcal{J} = \frac{\hbar}{2\omega_2\omega_3} \left\{ \frac{(\omega_2 + \omega_3)^2}{\omega_2 - \omega_3} (\Sigma_3 - \Sigma_2) + \frac{(\omega_2 - \omega_3)^2}{\omega_2 + \omega_3} (\Sigma_3 + \Sigma_2) \right\} \quad (43)$$

Here the anisotropic h.o. is characterised by the three frequencies ω_1, ω_2 and ω_3 along axes 1, 2 and 3 respectively, while the occupation factors Σ_1, Σ_2 and Σ_3 describe the sums

$$\Sigma_\kappa = \sum_{\nu-\text{occ.}} (n_\kappa + 1/2), \quad \kappa = 1, 2, 3 \quad (44)$$

extending over all the occupied orbits. Equation (43) for the nuclear moment of inertia should be completed by the selfconsistency condition

$$\omega_1 \Sigma_1 = \omega_2 \Sigma_2 = \omega_3 \Sigma_3 \quad (45)$$

and the volume conservation condition

$$\omega_1 \omega_2 \omega_3 = \omega_0^3 \sim 1/A \quad (46)$$

In this way the resulting moment of inertia \mathcal{J} from eq.(43) becomes effectively a function of several parameters

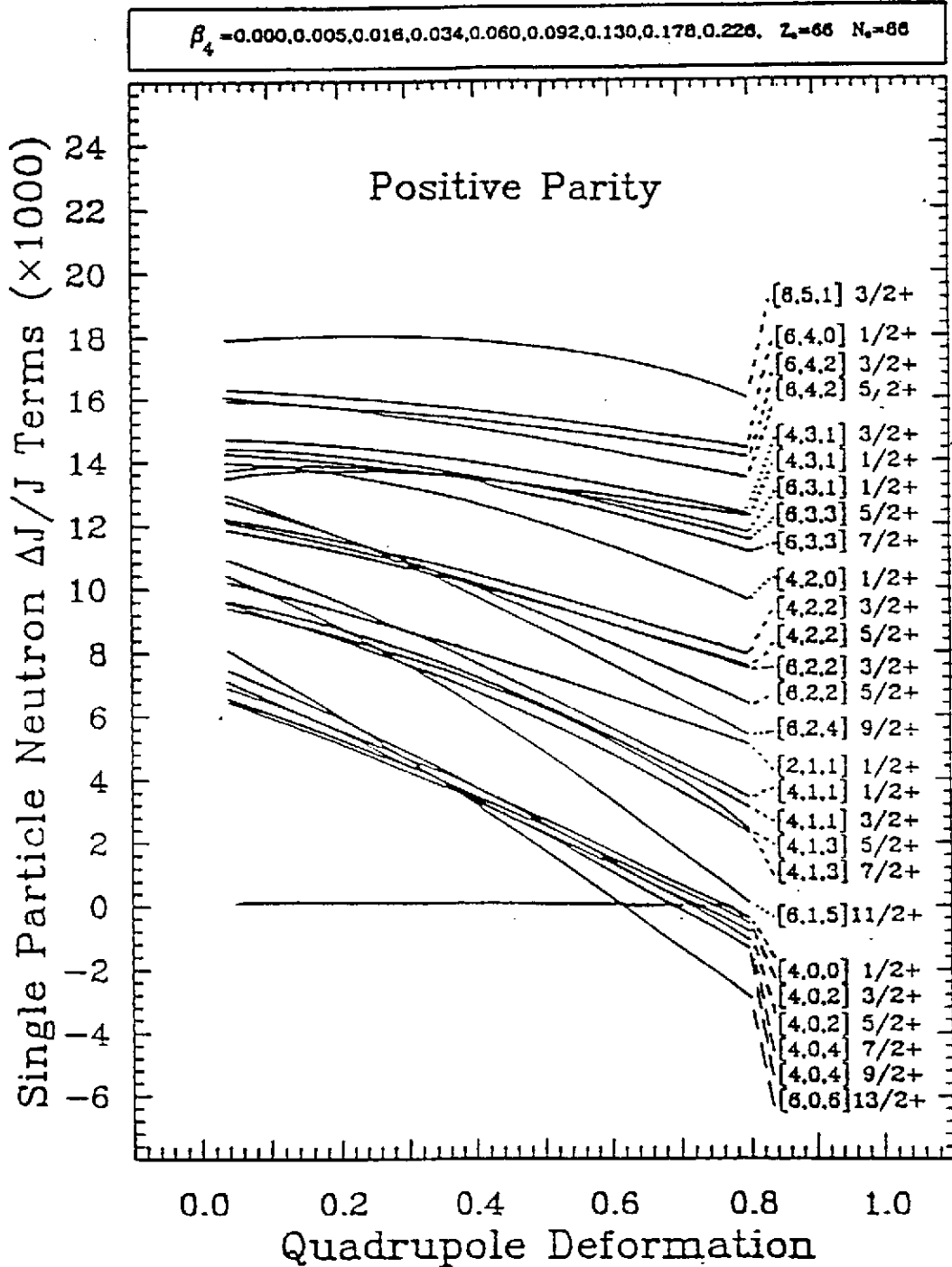
$$\mathcal{J} = F(A; \omega_1, \omega_2, \omega_3; \Sigma_1, \Sigma_2, \Sigma_3) \quad (47)$$

Now going over to the nearest odd- A nucleus the parameters change

$$\begin{aligned} A &\longrightarrow A + 1 \\ \omega_\kappa &\longrightarrow \omega_\kappa + \delta\omega_\kappa \\ \Sigma_\kappa &\longrightarrow \Sigma_\kappa + \delta\Sigma_\kappa = \Sigma_\kappa + (n_\kappa + 1/2) \end{aligned} \quad (48)$$

where the last term comes from the orbit occupied by the valence particle. Now, employing the perturbation theory and eliminating the quantities $\delta\omega_\kappa$ by means of the selfconsistency condition (45) and employing the volume conservation condition

Fig. 3.2



$E_{min} = -21.0$ (MeV), $E_{max} = -2.0$ STANDARD.

USM: 1DUDEK

(cf. eq. (46)) one can arrive at the expression for $\delta\mathcal{J}$ in the moment of inertia. Using the notation

$$\omega_1 = \omega_2 = \alpha\omega_3 = \Omega \quad (49)$$

$$\Sigma_1 = \Sigma_2 = \Sigma_3/\alpha = \Sigma \quad (50)$$

which is appropriate for the axially symmetric system we can express our formula as

$$\frac{\delta\mathcal{J}}{\mathcal{J}} = \frac{1}{3} \left\{ \frac{1}{A} - \frac{n_1 + 1/2}{\Sigma} - \frac{n_2 + 1/2}{\Sigma} \frac{\alpha^2 - 5}{\alpha^2 + 1} + \frac{n_3 + 1/2}{\Sigma} \frac{5\alpha^2 - 1}{\alpha(\alpha^2 + 1)} \right\} \quad (51)$$

Parameter α is related to deformation and takes the value $\alpha = 1$ for the spherical system, $\alpha = 2$ for the superdeformed configuration and $\alpha = 3$ for the hiperdeformed configuration.

There are two immediate conclusions that can be drawn from simple formula (51). First of all, the quantity $\delta\mathcal{J}/\mathcal{J}$ depends essentially on the quantum numbers n_1, n_2 and n_3 characterising the valence orbit. It can be seen that $\delta\mathcal{J}/\mathcal{J}$ is lowest for $n_3 = 0$. Secondly, quantity $\delta\mathcal{J}/\mathcal{J}$ decreases with deformation increasing.

A more realistic description of the effect has been attempted approximately in terms of the Woods-Saxon potential [25] by employing formula (51) averaged by the expansion coefficients of the eigenstates in the Woods-Saxon potential in terms of the eigenstates in the h.o. potential. The results provide a remarkable observation that quantity $\delta\mathcal{J}/\mathcal{J}$ is lowest for $n_3 = 0$ (next lowest value occurs for $n_3 = 1$) and drops down just for the superdeformed shape. This could perhaps explain why twin bands etc. that are observed at very large deformation do not show up at the usual deformations (say, at $\epsilon = 0.2-0.3$ for heavy nuclei). The plots of $\delta\mathcal{J}/\mathcal{J}$ versus α for $n_3 = 0, 1, 2, \dots$ are shown in Fig. 3.2. The appreciable decrease in $\delta\mathcal{J}$ described in this model can be understood as a cancellation between the volume effect and core-polarisation induced by the valence nucleon. Preliminary calculations [25] including also the effect of rotation do not seem to change the main conclusion of the above argument.

Summing up the above considerations we can conclude that the strange relations (31), (32) and (33) occur in the case when the valence orbit is characterised by the h.o. quantum number $n_3 = 0$ (or, at most $n_3 = 1$) i.e. when it corresponds to the nuclear density concentrated mostly near the equatorial plane (axes 1 and 2 in the nucleus).

As the results obtained above are only approximate further investigations in this domain are necessary.

Fig. 3.3a

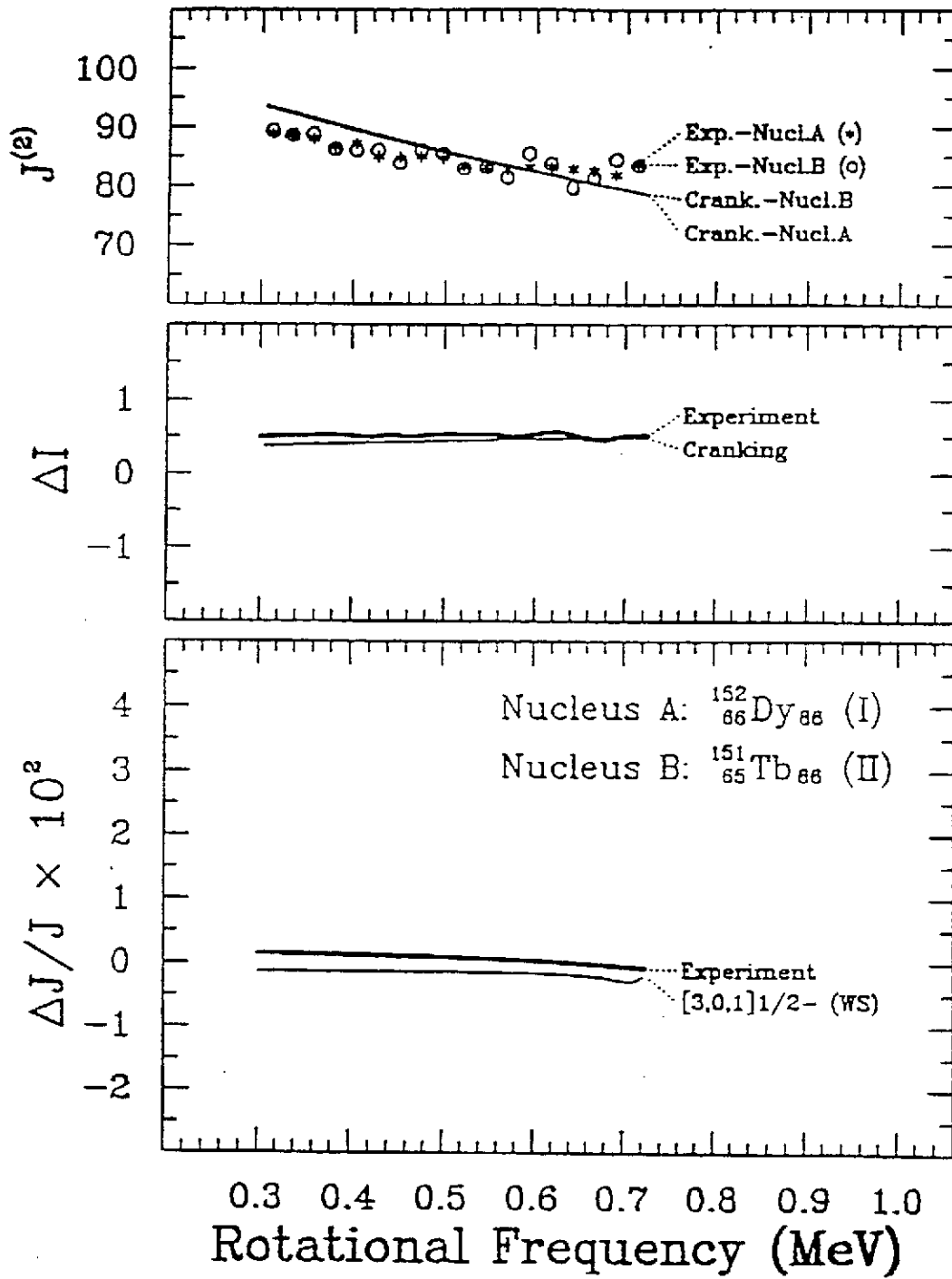
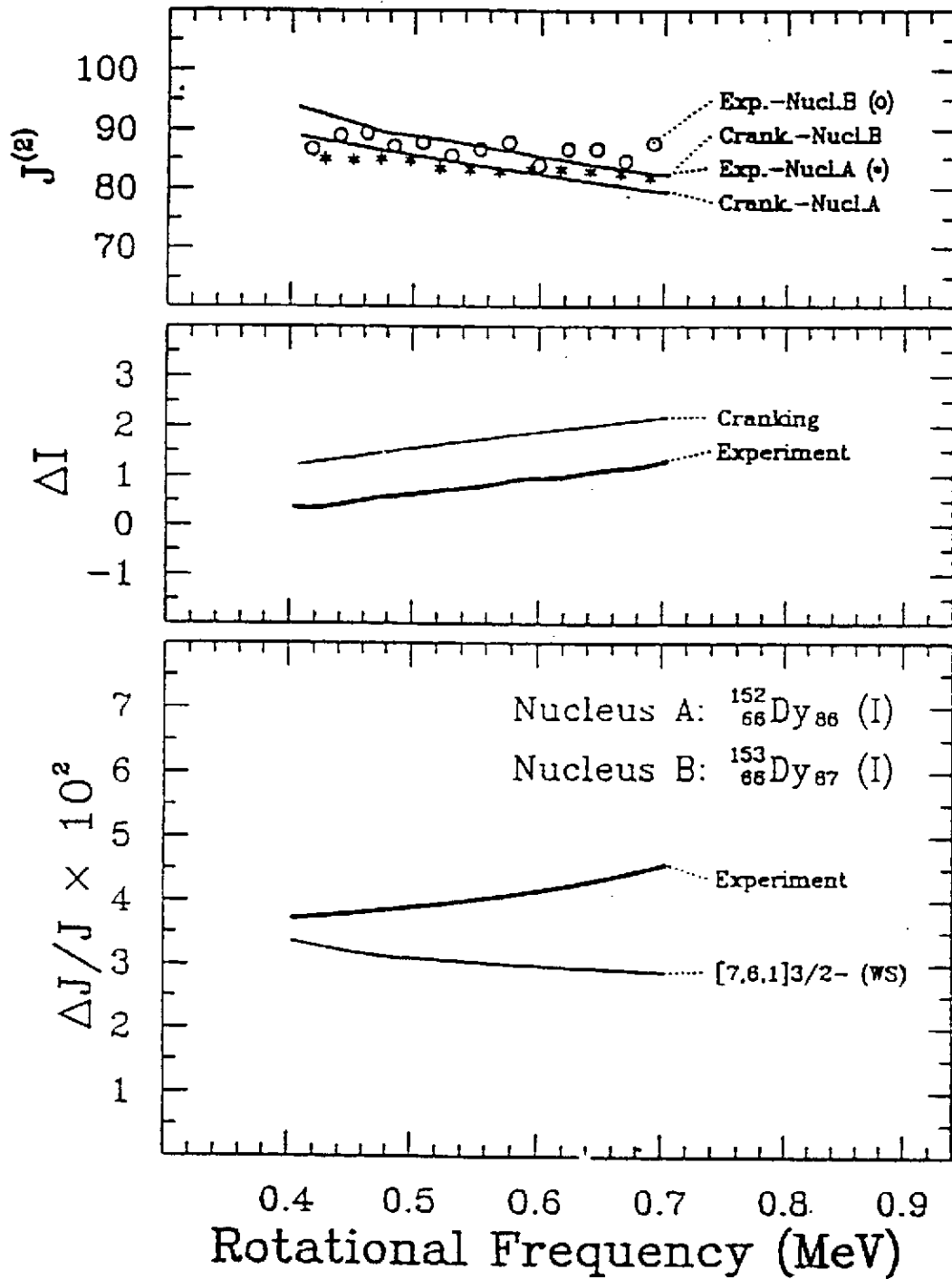


Fig. 3.3 b



Figs. 3.3a) and 3.3b) illustrate two cases; first with $n_3 = 1$ where $\delta\mathcal{J}/\mathcal{J}$ should be small and second with $n_3 = 6$ where no definite relation between the bands are expected.

References

1. W. Korten, J. Gerl, Ch. Ender, D. Habs, U.v. Helmold, H.W. Heyng, and D. Schwalm, Study of vibrational bands in ^{232}Th with the crystal ball spectrometer, Max Planck Institut für Kernphysik, preprint.
2. A. Bohr, Mat. Fys. Medd. Dan. Vid. Selsk. **26**, no 14 (1952).
3. A. Bohr and B.R. Mottelson, Mat. Fys. Medd. Dan. Vid. Selsk. **27**, no 16 (1953)
4. A. Bohr and B.R. Mottelson, Nuclear Structure, Vol.2, (1975), ed. W.A. Benjamin Inc. Reading, London, Amsterdam and Don Mills Ontario, Sydney, Tokyo.
5. D.R. Inglis, Phys.Rev., **96** (1954) 1059 and **97** (1955) 701.
6. L.D. Landau and E. Lifshitz, Mekhanika, 1965, Nauka, Moscow.
7. A. Bohr and B.R. Mottelson, Proc. Nobel Symposium 50, Örenäs, Physica Scripta **24** (1981) 71.
8. M.A.J. de Voigt, J. Dudek and Z. Szymanski, Rev. Mod. Phys. **55** (1983) 949.
9. A. Johnson, H. Ryde and S. Hjorth, Nucl. Phys. **A179** (1972) 753.
10. J. Dudek, current work, 1990.
11. S. Cohen, F. Plasil and W.J. Swiatecki, Ann. Phys., N.Y., **82** (1974) 557.
12. Z. Szymanski, lectures delivered at Ecole Joliot Curie de Physique Nucleaire, Bombannes, 1983.
13. J.D. Garrett, lecture delivered at Int.School on Heavy Ion Physics, Erice, Italy, 1986.
14. W. Nazarewicz, R. Wyss and A. Johnsson, Nucl. Phys. **A503** (1989) 285.

15. J. Dudek and T. Werner, to be published.
16. J.P. Elliot, Proc. Roy. Soc., **245** (1958) 128 and 562.
17. K.T. Hecht and A. Adler, Nucl. Phys. **A137** (1969) 129; R.D. Ratna Raju, J.P. Draayer and K.T. Hecht, Nucl.Phys. **A202** (1973) 433.
18. A. Bohr, I. Hamamoto and B.R. Mottelson, Phys. Scripta, **26** (1982) 267.
19. J. Dudek, W. Nazarewicz, Z. Szymanski and G. Leander, Phys. Rev. Lett. **59** (1987) 1405.
20. T. Byrski, F.A. Beck, D. Curien, C. Schuck, P. Fallon, A. Alderson, I. Ali, M.A. Bentley, A.M. Bruce, P.D. Forsyth, D. Howe, J.W. Roberts, J.F. Sharpey-Schaffer, G. Smith and P.J. Twin, Phys. Rev. Letters **64** (1990) 1650.
21. W.Nazarewicz, P.J. Twin, P. Fallon and J.D. Garrett, Phys. Rev. Lett. **64** (1990) 1654.
22. F.S. Stephens et al. Phys. Rev. Lett. **64** (1990) 2623.
23. F.S. Stephens et al. Phys. Rev. Lett. **65** (1990) 301.
24. I. Ragnarsson in Proc. of Int. Conf. on Nucl. Struct. in the Nineties, Oak Ridge, Tennessee, April, 1990.
25. J. Dudek, Z. Szymanski and T. Werner, to be published.
26. A. Bohr and B.R. Mottelson, Mat. Fys, Medd. Dan. Vid. Selsk. **30** no 1 (1955).